



**HAL**  
open science

## MC-PDNET: Deep unrolled neural network for multi-contrast mr image reconstruction from undersampled k-space data

Kumari Pooja, Zaccharie Ramzi, Chaithya Giliyar Radhakrishna, Philippe Ciuciu

### ► To cite this version:

Kumari Pooja, Zaccharie Ramzi, Chaithya Giliyar Radhakrishna, Philippe Ciuciu. MC-PDNET: Deep unrolled neural network for multi-contrast mr image reconstruction from undersampled k-space data. ISBI 2022 - IEEE International Symposium on Biomedical Imaging 2022, IEEE, Mar 2022, Kolkata, India. hal-03389390

**HAL Id: hal-03389390**

**<https://inria.hal.science/hal-03389390>**

Submitted on 21 Oct 2021

**HAL** is a multi-disciplinary open access archive for the deposit and dissemination of scientific research documents, whether they are published or not. The documents may come from teaching and research institutions in France or abroad, or from public or private research centers.

L'archive ouverte pluridisciplinaire **HAL**, est destinée au dépôt et à la diffusion de documents scientifiques de niveau recherche, publiés ou non, émanant des établissements d'enseignement et de recherche français ou étrangers, des laboratoires publics ou privés.



Distributed under a Creative Commons Attribution 4.0 International License

# MC-PDNET: DEEP UNROLLED NEURAL NETWORK FOR MULTI-CONTRAST MR IMAGE RECONSTRUCTION FROM UNDERSAMPLED K-SPACE DATA

Kumari Pooja<sup>(1,2)</sup>, Zaccharie Ramzi<sup>(1,2,3)</sup>, Chaithya GR<sup>(1,2)</sup> and Philippe Ciuciu<sup>(1,2)</sup>

<sup>(1)</sup> CEA, Joliot, NeuroSpin, Université Paris-Saclay, F-91191 Gif-sur-Yvette, France.

<sup>(2)</sup> Inria, Parietal, Université Paris-Saclay, F-91120 Palaiseau, France.

<sup>(3)</sup> AIM, CEA, CNRS, Université Paris-Saclay, Université Paris Diderot.

## ABSTRACT

Multi-contrast (MC) MR images are similar in structure and can leverage anatomical structure to perform joint reconstruction especially from a limited number of k-space data in the Compressed Sensing (CS) setting. However CS-based multi-contrast image reconstruction has shown limited performance in these highly accelerated regimes due to the use of hand-crafted group sparsity priors. Deep learning can improve outcomes by learning the joint prior across multiple weighting contrasts. In this work, we extend the primal-dual neural network (PDNet) in the multi-contrast sense. We propose a MC-PDNet architecture which takes full advantage of multi-contrast information. Using an in-house database consisting of images from  $T_2$ TSE,  $T_2^*$ GRE and FLAIR contrasts acquired in 65 healthy volunteers, we performed a retrospective study from 4-fold under-sampled data. It was shown that MC-PDNet improves image quality by at least 1dB in PSNR for each contrast individually in comparison with PD-Net and U-Net architectures.

**Index Terms**— MRI reconstruction, Deep learning, Multi-contrast imaging.

## 1. INTRODUCTION

Magnetic Resonance Imaging (MRI) is one of the most powerful imaging techniques used to probe soft tissues within the human body, especially those of the human brain. Included within a clinical MRI exam, the physician has the option to exploit several contrast-weighted MR images of the same anatomy including  $T_1$ ,  $T_2$ ,  $T_2^*$ , FLAIR, etc., to maximize diagnostic accuracy. The corresponding data is collected sequentially and the MR images reconstructed independently. In the interest of high-throughput and fast MR imaging, Compressed Sensing (CS) has been used for more than a decade to reduce scan times [1] but at the expense of longer iterative image reconstruction. CS MRI reconstruction has been successfully used in hundreds of papers with several significant contributions in the specific domain of multi-contrast (MC) image reconstruction [2–4].

This success is attributed to the capacity of viewing multiple imaging contrasts of the same underlying anatomy that share similar structures, as illustrated in Fig. 1 on a single brain. Leveraging this shared information in an optimal way, however, requires designing hand-crafted joint sparsity priors that go beyond the single sparsity currently in use in classical MR image reconstruction. Such advanced priors combine two ingredients: First, the choice of a sparse transform or representation (e.g. graph-based wavelet [3,4]) and second, the definition of the most appropriate penalty term (e.g. group-LASSO [5] or OSCAR [6,7]) to combine multi-contrast information. One method to address these issues is to learn the prior

itself in a data-driven manner. Deep learning (DL) offers the ideal framework by which to achieve this goal and has actually already been successfully used for MR image reconstruction [8–12], notably see the benchmark paper published in [13].

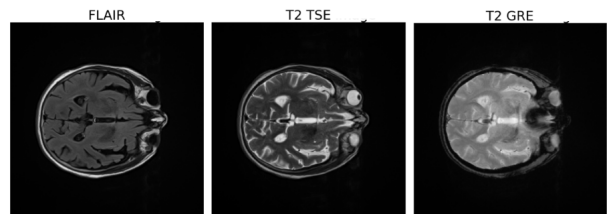


**Fig. 1.** Multi-contrast MR images (FLAIR,  $T_2$  Turbo spin echo -TSE and  $T_2$  Gradient Recalled Echo) sharing similar structures.

The existing literature on DL for MC-MRI reconstruction comprises two contributions. The first, called joint variational network (jVN) [14], has basically extended the variational neural network originally introduced for single contrast multi-coil MR image reconstruction from Cartesian under-sampled data [10]. The second contribution entails a deep information sharing network to exploit the structural similarity across imaging contrasts [15]. However, in this work the architecture is based on a cascade of networks and dense connections hence significantly affecting the memory footprint of the architecture on GPU resources.

In the present work, we propose an extension of the PD-Net architecture to MC-MRI reconstruction. This cross-domain architecture was initially introduced for tomographic image reconstruction [16], tested as such on MRI [17] and then further extended as XPD-Net to multi-coil MR image reconstruction [13]<sup>1</sup>. As this architecture secured the second place at the 2020 brain fastMRI challenge [18], it naturally holds great promise for multi-contrast MR image reconstruction. In this work we introduce the MC-PDNet architecture that accumulates imaging contrasts as a supplementary channel dimension which allows us to share weights in the CNN across contrasts and limit the memory footprint. Moreover, for this proof of concept the focus will only pertain to single-coil 2D imaging and Cartesian data even though it could be easily extended to 3D imaging and for non-Cartesian readout following the ideas proposed in the NC-PDNet extension [19]. Finally, we present the results of retrospective studies performed on 4-fold under-sampled magnitude-only data extracted from the above described in-house database that was constructed for analyzing the effects of aging on the brain. On

<sup>1</sup>Here, X stands for a wildcard and means that XPD-Net can internally host any CNN in the k-space and image domains.

8 unseen test subjects, we show how MC-PDNet provides improved image quality in comparison to single contrast DL architectures (PDNet, U-Net).

## 2. MODELING

In this section, we introduce a basic formulation of CS MC-MRI reconstruction that will be reused afterwards in the DL framework for handling the multi-contrast data consistency term.

### 2.1. Multi-contrast CS MR image reconstruction

Under multi-contrast setting with  $C$  contrasts, the stacked MR images can be modeled by  $\mathbf{X} = (\mathbf{x}_c)_{c=1}^C$  with  $\mathbf{x}_c \in \mathbb{C}^{N \times N} \forall c \in [1, C]$  being a 2D MR image per contrast. Let  $M$  be the number of measurements in the Fourier domain with  $M \ll N \times N$  as we operate in the CS setting. Then the acquired k-space data  $\mathbf{y}_c$  associated with the  $c^{\text{th}}$  contrast<sup>2</sup> is given by the following idealized forward model:

$$\mathbf{y}_c = \mathbf{F}_{\Omega_c} \mathbf{x}_c, \quad \forall c = 1 \dots, C \quad (1)$$

where  $\mathbf{F}_{\Omega_c}$  is the undersampled Fourier operator. In our case of Cartesian under-sampling with masks  $\Omega_c$ , we get:  $\mathbf{F}_{\Omega_c} = \Omega_c \mathbf{F}$ , where  $\mathbf{F}$  is the fast Fourier transform. Note that different under-sampling masks may be used across the multiple imaging contrasts for boosting the signal-to-noise ratio or recovering high frequencies in a complementary manner.

Let  $\Psi_s$  be an orthonormal transform (e.g. a wavelet transform) that sparsifies  $\mathbf{x}_c$  in the sense that  $\mathbf{z}_c = \Psi_s \mathbf{x}_c$  is a  $s_c$ -sparse vector, i.e. its support contains at most  $s_c$  non-zero coefficients. For the sake of simplicity, we assume that  $\mathbf{z}_c \in \mathbb{C}^{n_\Psi}$ ,  $\forall c$  and denote  $\mathbf{Z} = [\mathbf{z}_1, \mathbf{z}_2 \dots, \mathbf{z}_C]^T \in \mathbb{C}^{n_\Psi \times C}$ . A convenient approach to perform CS MC-MRI reconstruction is to seek the global minimizer of the following convex but non-smooth cost function, which was introduced in the calibrationless multi-coil MRI reconstruction [7]:

$$\hat{\mathbf{Z}} = \underset{\mathbf{Z} \in \mathbb{C}^{n_\Psi \times C}}{\operatorname{argmin}} \frac{1}{2} \sum_{c=1}^C \|\mathbf{y}_c - \mathbf{F}_{\Omega_c} \Psi_s^* \mathbf{z}_c\|_2^2 + \lambda g(\mathbf{Z}). \quad (2)$$

This formulation combines the  $\ell_2$  multi-contrast data consistency term with a group-sparsity promoting term  $g(\cdot)$ . If we assume that the same sparsity structure exists across the multiple contrasts, the group Least Absolute Shrinkage and Selection Operator or group-LASSO penalty [5] can be used for  $g$ . However, such sparsity structure may vary across contrasts, leading to the use of a more flexible choice for  $g$  like OSCAR penalty term (Octagonal Shrinkage and Clustering Algorithm for Regression) [7]. In [7, 20], a primal-dual optimization method proposed by Condat-Vũ was used to solve (2). It relies on the closed form expression of the proximity operator of  $g$ , which is available in the case of group-LASSO and OSCAR regularization (see [7, 20] for details).

After convergence, the multi-contrast images can be reconstructed as follows:  $\forall c \in [1, C]$ ,  $\hat{\mathbf{x}}_c = \Psi_s^* \hat{\mathbf{z}}_c$ . However, CS MC-MRI reconstruction is more demanding in terms of computing time as compared single contrast reconstruction. Additionally, there is no guarantee that the hand-crafted prior for CS MC-MRI reconstruction is optimal for the set of imaging contrasts under study as no information about the data is injected. Although dictionary learning [21] has helped to tackle this limitation and build up data-informed priors, this is done at the cost of computing time.

<sup>2</sup>Here we ignore  $B_0$  inhomogeneities artifacts and  $T_2$ -decay effects.

The recent rise of large imaging databases and DL has facilitated the emergence of new MRI reconstruction algorithms which efficiently use GPU processing to speed up the reconstruction times at inference (i.e. test time) and improve the image quality at the same time. Hereafter, we detail how we can benefit from cross-domain DL architectures as the most promising approaches to combine the data consistency term involved in (2) with a learned denoiser that corresponds to the proximity operator of the prior  $g$ .

### 2.2. Multi-contrast PDNet : MC-PDNet

In our study, we have focused on the primal dual network (PDNet) which unrolls the Primal Dual Hybrid Gradient (PDHG) algorithm [22]. In this architecture, proximal operators are replaced by convolutional operators. Additionally, we carry a buffer between the different unrolled iterations ( $N_c = 12$ ) rather than a single multi-contrast image estimate. This buffer allows us to learn a nonlinear acceleration scheme as explained in [23].

In this work, we adapted the originally developed multi-coil XPDNet [13] to MC-MRI. The coil dimension in the network was replaced with the contrast dimension. Hence, the input to our network is the stacked multi-contrast k-space data  $\mathbf{Y} = (\mathbf{y}_i)_{i=1}^C$ . We discarded the parts of the network related to the sensitivity map refinement. We carried out a vectorized Fourier transform on all data to alternate between the image space and k-space. We present this multi-contrast PDNet (MC-PDNet) in Fig. 2. The components of this network include:

- **Buffer State:** To include the buffer state for each contrast image, we have taken the outer dimension as buffer dimension. As input dimensions will be  $n_{\text{sl}} \times C \times H \times W \times B_{\text{dim}}$  with  $n_{\text{sl}}$  the number of slices,  $C$  the number of contrasts,  $H$  and  $W$  the respective height and width of convolution filters,  $B_{\text{dim}}$  will define the buffer size (here,  $B_{\text{dim}} = 5$ ).
- **Multi-contrast Fourier transform:** Under-sampled FFT and adjoint FFT were applied to each contrast using the same mask  $\Omega_c = \Omega, \forall c$  for the sake of simplicity while alternating between primal (i.e. image) and dual (i.e. k-space) domains.
- **Multi-contrast Data consistency:** Here, we extended to multi-contrast imaging the measurements residual as done for the primal-only version of the PDNet and in the winning solution of the fastMRI challenge [24]:  $f(\mathbf{Y}, \mathbf{Y}_k, \Omega) = \mathbf{Y} - M_\Omega \mathbf{Y}_k$  where  $M_\Omega$  is the multi-contrast stacked masking operator and  $\mathbf{Y}_k$  is the full k-space data at the  $k^{\text{th}}$  unrolled iteration of MC-PDNet.
- **Joint metrics for training:** We have given equal weight to each contrast during the training stage. The metrics used for evaluating the networks are as Peak signal-to-noise ratio (PSNR) and structural similarity index (SSIM). They are computed over the 35 middle slices of each volume and then averaged across contrasts, that is the dynamic range (used for the computation of PSNR and SSIM) is computed on the whole volume. The parameters and definitions used are the same as in the fastMRI paper [25].

By doing so, the MC-PDNet architecture jointly learns from each contrast and improves the overall reconstruction of each contrast.

## 3. EXPERIMENTAL SETUP

### 3.1. Data

In this study, we used 2D MR imaging dataset from Senior protocol acquired on a clinical 3T MR system (Magnetom Prisma<sup>FIT</sup>, Siemens Healthcare, Erlangen, Germany) with a 64-channel head/neck

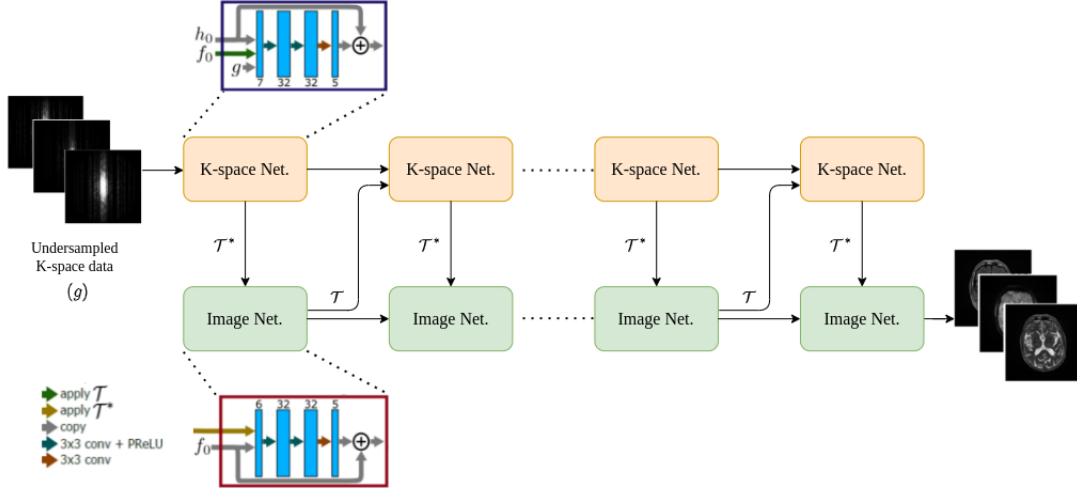


**Fig. 2.** Description of MC-PDNet (reference from [16]): Input data  $g$  are retrospective multi-contrast under-sampled k-space data. Here, the red and blue boxes represent the primal and dual networks, respectively.  $h_0$  and  $f_0$  represent the initial k-space and image respectively which are set as zero-valued tensors.  $\mathcal{T}$  stands for the multi-contrast Fourier operator while  $\mathcal{T}^*$  represents the inverse multi-contrast Fourier operator. Final output is the stacked multi-contrast reconstructed image.

coil array at NeuroSpin, CEA Paris Saclay, with an in-plane resolution of 1mm and slice thickness of 2.5mm. The 2D MR image size was  $256 \times 256$  and we had 70 slices per volume. In this study we used the FLAIR,  $T_2^*$  GRE and  $T_2$  TSE contrasts in each volunteer and we left  $T_1$  images aside as they did not match in size. The full dataset had 65 volumes, which was split into training and validation as 80% / 20%. 8 additional volumes were used for testing. We used magnitude-only images in DICOM format due to the absence of raw k-space data to take complex-valued images. We retrospectively under-sampled the Fourier space of these images using a 1D variable density Cartesian sampling along the phase encoding direction (see Fig. 3). For this study, we used an acceleration factor (AF) of 4 (i.e. 25% of k-space data were used). We fully sampled the 8% in the center of k-space to preserve the contrasts and then under-sampled the higher frequencies randomly.

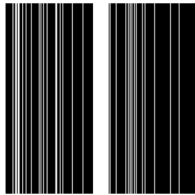


**Fig. 3.** Sampling mask ( $256 \times 256$ ) used to generate under-sampled k-space data.

### 3.2. Training details

Our model was trained with batch size of 1 with mean absolute error (MAE) as loss, at a learning rate of  $10^{-3}$  using the ADAM optimizer. We used a learning rate scheduler which reduced the learning rate by a factor of 0.5 if the network didn't improve for 15 consecutive epochs. We trained our network for 100 epochs on a Quadro RTX8000 GPU with 48GB DRAM. The entire training process took us 30 minutes.

## 4. RESULTS

We compared the proposed MC-PDNet against (i) zero-filled inverse Fourier transform as a naive baseline, (ii) U-Net [26] with similar filters and (iii) PDNet. Each of these networks was learned on each contrast separately. Such comparison aims to understand if the proposed architecture utilizes the complementary information conveyed by other imaging contrasts.

**Table 1.** Performances on 8 test individuals at 3T ( $T_2^*$  GRE).

Model	PSNR-mean (std) / SSIM-mean (std)	# params
Zero Filled	30.13 (1.45) / 0.8233 (0.023)	0
UNET	35.34 (1.61) / 0.9401 (0.010)	481801
PDNet	40.55 (2.37) / 0.9763 (0.007)	381936
MC-PDNet	<b>41.3 (1.32) / 0.9813 (0.004)</b>	381936

**Table 2.** Performances on 8 test individuals at 3T ( $T_2$  FLAIR).

Model	PSNR-mean (std) / SSIM-mean (std)	# params
Zero Filled	26.38 (1.04) / 0.717 (0.022)	0
UNET	32.62 (0.94) / 0.9304 (0.008)	481801
PDNet	38.52 (1.89) / 0.9747 (0.007)	381936
MC-PDNet	<b>41.71 (1.75) / 0.9846 (0.003)</b>	381936

**Table 3.** Performances on 8 test individuals at 3T ( $T_2$  TSE).

Model	PSNR-mean (std) / SSIM-mean (std)	# params
Zero Filled	25.43 (0.96) / 0.6812 (0.017)	0
UNET	30.93 (1.65) / 0.929 (0.014)	481801
PDNet	39.05 (1.92) / 0.9829 (0.004)	381936
MC-PDNet	<b>40.0 (2.41) / 0.9847 (0.006)</b>	381936

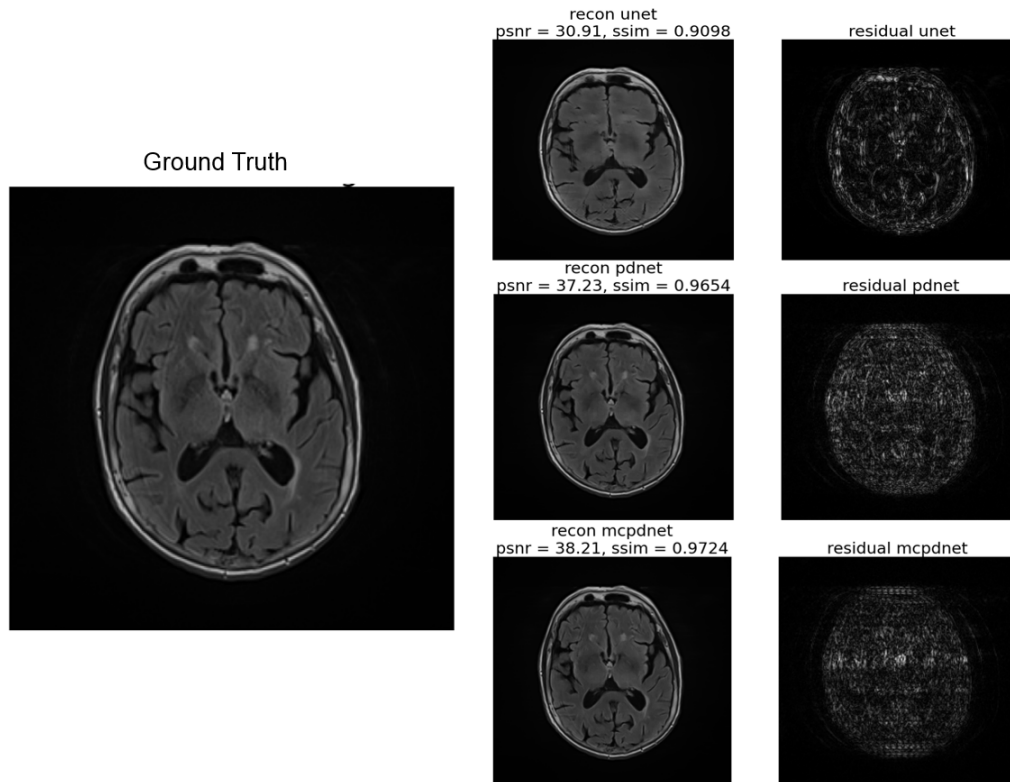


**Fig. 4.** Reconstruction result for  $T_2$  FLAIR image (35th slice, one of the subject from test set), first column is the ground truth, second column shows reconstructed image from each model and third column depicts the residual between ground truth and reconstructed image

#### 4.1. Quantitative results

We present the PSNR and SSIM scores for  $T_2^*$  GRE,  $T_2$  FLAIR and  $T_2$  TSE in Tab. 1, 2, 3 respectively. We observe that MC-PDNet clearly outperforms all the competing methods with SSIM scores reaching up to 0.98 as compared to 0.93-0.94 in U-Net and 0.97 in PDNet. Specifically, improved performance of MC-PDNet architecture over PDNet was particularly observed in PSNR. This strongly suggests that the trained multi-contrast network utilizes complementary information conveyed by the other data/contrasts.

#### 4.2. Qualitative results

To understand the performance of MC-PDNet visually, we present a single reconstructed slice and residual from FLAIR contrast in the test set in Fig. 4. We clearly observe that MC-PDNet provides the closest image to the ground truth as its residual map retains much lesser structures. This is also corroborated with its higher SSIM and PSNR scores of 0.9724 and 38.21, respectively.

### 5. CONCLUSION AND DISCUSSIONS

In this study, we proposed a novel extension of the PD-Net architecture, called MC-PDNet, to address multi-contrast MR image reconstruction. We found that such a network can exploit complementary information conveyed by other imaging contrasts through the multiple k-space data. The information is actually shared in the image domain where the MR images are stacked as multiple channels with common weights, thereby improving image quality. MC-

PDNet was evaluated retrospectively in the Cartesian setting on 4-fold under-sampled multi-contrast data. However future prospect will involve the extension to non-Cartesian acquisition by mimicking the NC-PDNet [19] and possibly the validation on larger public databases (e.g. OASIS-3).

### 6. COMPLIANCE WITH ETHICAL STANDARDS

This Senior protocol involves a total of 100 healthy volunteers scanned longitudinally once a year to understand the dynamics of aging for human brain. The protocol has been approved by local and national ethical committees, and written consent was obtained from the volunteers.

### 7. ACKNOWLEDGMENTS

We have no acknowledgments to disclose.

### 8. REFERENCES

- [1] Michael Lustig, David Donoho, and John M. Pauly, "Sparse MRI: The application of compressed sensing for rapid MR imaging," *Magnetic Resonance in Medicine*, vol. 58, no. 6, pp. 1182–1195, 2007.
- [2] Junzhou Huang, Chen Chen, and Leon Axel, "Fast multi-contrast MRI reconstruction," *Magnetic resonance imaging*, vol. 32, no. 10, pp. 1344–1352, 2014.

- [3] Zongying Lai, Xiaobo Qu, Hengfa Lu, Xi Peng, Di Guo, Yu Yang, Gang Guo, and Zhong Chen, "Sparse MRI reconstruction using multi-contrast image guided graph representation," *Magnetic resonance imaging*, vol. 43, pp. 95–104, 2017.
- [4] Zongying Lai, Xinlin Zhang, Di Guo, Xiaofeng Du, Yonggui Yang, Gang Guo, Zhong Chen, and Xiaobo Qu, "Joint sparse reconstruction of multi-contrast MRI images with graph based redundant wavelet transform," *BMC medical imaging*, vol. 18, no. 1, pp. 1–16, 2018.
- [5] Angshul Majumdar and Rabab K Ward, "Calibration-less multi-coil MR image reconstruction," *Magnetic resonance imaging*, vol. 30, no. 7, pp. 1032–1045, 2012.
- [6] Howard D Bondell and Brian J Reich, "Simultaneous regression shrinkage, variable selection, and supervised clustering of predictors with oscar," *Biometrics*, vol. 64, no. 1, pp. 115–123, 2008.
- [7] Loubna El Gueddari, Philippe Ciuciu, Emilie Chouzenoux, Alexandre Vignaud, and J-C Pesquet, "Calibrationless oscar-based image reconstruction in compressed sensing parallel mri," in *2019 IEEE 16th International Symposium on Biomedical Imaging (ISBI 2019)*. IEEE, 2019, pp. 1532–1536.
- [8] Yan Yang, Jian Sun, Huibin Li, Zongben Xu, Jian Sun, and Zongben Xu, "Deep ADMM-net for compressive sensing MRI," in *Neural Information Processing Systems*, 2016, number Nips, pp. 10–18.
- [9] Bo Zhu, Jeremiah Z. Liu, Stephen F. Cauley, Bruce R. Rosen, and Matthew S. Rosen, "Image reconstruction by domain-transform manifold learning," *Nature*, vol. 555, no. 7697, pp. 487–492, 03 2018.
- [10] Kerstin Hammernik, Teresa Klatzer, Erich Kobler, Michael P Recht, Daniel K Sodickson, Thomas Pock, and Florian Knoll, "Learning a variational network for reconstruction of accelerated mri data," *Magnetic resonance in medicine*, vol. 79, no. 6, pp. 3055–3071, 2018.
- [11] Jo Schlemper, Jose Caballero, Joseph V Hajnal, Anthony Price, and Daniel Rueckert, "A Deep Cascade of Convolutional Neural Networks for MR Image Reconstruction," *IEEE Transactions on Medical Imaging*, vol. 37, no. 2, pp. 491–503, 2018.
- [12] Dongwook Lee, Jaejun Yoo, Sungho Tak, and Jong Chul Ye, "Deep residual learning for accelerated MRI using magnitude and phase networks," *IEEE Transactions on Biomedical Engineering*, vol. 65, no. 9, pp. 1985–1995, 2018.
- [13] Zaccharie Ramzi, Philippe Ciuciu, and Jean-Luc Starck, "Benchmarking MRI reconstruction neural networks on large public datasets," *Applied Sciences*, vol. 10, no. 5, pp. 1816, 2020.
- [14] Daniel Polak, Stephen Cauley, Berkin Bilgic, Enhao Gong, Peter Bachert, Elfar Adalsteinsson, and Kawin Setsompop, "Joint multi-contrast variational network reconstruction (jvn) with application to rapid 2d and 3d imaging," *Magnetic resonance in medicine*, vol. 84, no. 3, pp. 1456–1469, 2020.
- [15] Liyan Sun, Zhiwen Fan, Xueyang Fu, Yue Huang, Xinghao Ding, and John Paisley, "A deep information sharing network for multi-contrast compressed sensing mri reconstruction," *IEEE Transactions on Image Processing*, vol. 28, no. 12, pp. 6141–6153, 2019.
- [16] Jonas Adler and Ozan Öktem, "Learned primal-dual reconstruction," *IEEE transactions on medical imaging*, vol. 37, no. 6, pp. 1322–1332, 2018.
- [17] Jing Cheng, Haifeng Wang, Leslie Ying, and Dong Liang, "Model learning: Primal dual networks for fast mr imaging," in *International Conference on Medical Image Computing and Computer-Assisted Intervention*. Springer, 2019, pp. 21–29.
- [18] Matthew J Muckley, Bruno Riemenschneider, Alireza Radmanesh, Sunwoo Kim, Geunu Jeong, Jingyu Ko, Yohan Jun, Hyungseob Shin, Dosik Hwang, Mahmoud Mostapha, et al., "Results of the 2020 fastMRI challenge for machine learning MR image reconstruction," *IEEE transactions on medical imaging*, vol. 40, no. 9, pp. 2306–2317, 2021.
- [19] Zaccharie Ramzi, G Chaithya, Jean-Luc Starck, and Philippe Ciuciu, "NC-PDNet: a density-compensated unrolled network for 2D and 3D non-Cartesian MRI reconstruction," 2021.
- [20] Laurent Condat, "A primal–dual splitting method for convex optimization involving Lipschitzian, proximable and linear composite terms," *Journal of Optimization Theory and Applications*, vol. 158, no. 2, pp. 460–479, Aug. 2013.
- [21] Saiprasad Ravishankar and Yoram Bresler, "Magnetic Resonance Image Reconstruction from Highly Undersampled K-Space Data Using Dictionary Learning," *IEEE Transactions on Medical Imaging*, vol. 30, no. 5, pp. 1028–1041, 2011.
- [22] Antonin Chambolle and Thomas Pock, "A First-Order Primal-Dual Algorithm for Convex Problems with Applications to Imaging," pp. 120–145, 2011.
- [23] Jonas Adler and Ozan Oktem, "Solving ill-posed inverse problems using iterative deep neural networks," *Inverse Problems*, vol. 33, no. 12, pp. 1–24, 2017.
- [24] Nicola Pezzotti, Sahar Yousefi, Mohamed S Elmahdy, Jeroen Van Gemert, Christophe Schülke, Mariya Doneva, Tim Nielsen, Sergey Kastrulin, Boudewijn P F Lelieveldt, Matthias J P Van Osch, Elwin De Weerd, and Marius Starving, "An Adaptive Intelligence Algorithm for Undersampled Knee MRI Reconstruction: Application to the 2019 fastMRI Challenge," Tech. Rep., 2019.
- [25] Jure Zbontar, Florian Knoll, Anuroop Sriram, Tullie Murrell, Zhengnan Huang, Matthew J Muckley, Aaron Defazio, Ruben Stern, Patricia Johnson, Mary Bruno, et al., "fastmri: An open dataset and benchmarks for accelerated mri," *arXiv preprint arXiv:1811.08839*, 2018.
- [26] Olaf Ronneberger, Philipp Fischer, and Thomas Brox, "U-net: Convolutional networks for biomedical image segmentation," in *International Conference on Medical image computing and computer-assisted intervention*. Springer, 2015, pp. 234–241.